engineering proceedings

MDPI

Proceeding Paper

Antioxidant Activity of Ablated CeO_2 Nanoparticles with Narrow-Size Distribution †

Vladimir Mamontov [1,*], Maksim Pugachevskii [1], Petr Snetkov [2] and Ratneshwar Kumar Ratnesh [3]

[1] Department of Nanotechnology, Microelectronics, General and Applied Physics, Regional Center of Nanotechnology, Southwest State University, 50 Years of October Street, 94, 305040 Kursk, Russia; pmaximal@mail.ru
[2] Institute of Advanced Data Transfer Systems, ITMO University, Kronverkskiy Prospekt, 49, bldg. A, 197101 Saint Petersburg, Russia; ppsnetkov@itmo.ru
[3] Department of Electronics and Communication Engineering, Meerut Institute of Engineering and Technology, Meerut 250005, Uttar Pradesh, India; ratneshwar.ratnesh@miet.ac.in
* Correspondence: vladimir-mamontov2013@yandex.ru
† Presented at the 5th International Electronic Conference on Applied Sciences, 4–6 December 2024; https://sciforum.net/event/ASEC2024.

Abstract: A method for the synthesis of nanodispersed aqueous solutions based on ablated cerium dioxide nanoparticles with a narrow-size distribution has been developed, and their physicochemical properties have been investigated. The nanoparticle sizes of CeO_2 were analyzed using atomic force microscopy and small-angle X-ray scattering. The dependence of the electronic structure of ablated cerium dioxide nanoparticles on their size was established. The influence of the size factor on the antioxidant properties of the obtained particle size groups was investigated.

Keywords: cerium dioxide nanoparticles; structural defects; spectrophotometry; reaction rate; laser ablation; photocatalytic reaction

1. Introduction

Cerium dioxide nanoparticles exhibit antioxidant properties, enabling them to neutralize free radicals and ROS [1,2]. Laser ablation produces cerium dioxide nanoparticles with surface structural defects that determine their antioxidant properties [3]. Due to cerium's ability to easily change oxidation states ($Ce^{3+} \leftrightarrow Ce^{4+}$), an antioxidant cycle capable of neutralizing harmful radicals is established on the nanoparticle surface [4]. The activity of these nanoparticles can be significantly enhanced by forming them under highly nonequilibrium thermal conditions, which leads to enrichment with functional structural defects, substantially improving their physicochemical properties [5].

The authors of [6] note that various factors, such as shape, size, and structure, can influence the physicochemical properties of nanoparticles. Studies [7–9] have demonstrated that nanodispersed solutions of ablated cerium dioxide particles after centrifugation exhibit pronounced antioxidant properties both in the Fenton reaction and in photocatalytic reactions. According to [10], cerium dioxide nanoparticles centrifuged at different speeds possess reduced stoichiometry, indicating a high concentration of structural defects such as oxygen vacancies in ablated cerium dioxide nanoparticles. The aim of this study is to obtain stabilized nanodispersed solutions of ablated cerium dioxide particles with a narrow-size distribution with specified maximum and minimum particle sizes. Since laser ablation produces particles in a wide size range, it is of particular interest to separate nanodispersed

check for updates

Academic Editor: Nunzio Cennamo

Published: 27 April 2025

Citation: Mamontov, V.; Pugachevskii, M.; Snetkov, P.; Ratnesh, R.K. Antioxidant Activity of Ablated CeO_2 Nanoparticles with Narrow-Size Distribution. *Eng. Proc.* **2025**, *87*, 55. https://doi.org/10.3390/engproc2025087055

Copyright: © 2025 by the authors. Licensee MDPI, Basel, Switzerland. This article is an open access article distributed under the terms and conditions of the Creative Commons Attribution (CC BY) license (https://creativecommons.org/licenses/by/4.0/).

solutions of ablated cerium dioxide particles into narrow-size groups to investigate the dependence of their antioxidant properties on particle size.

2. Methods and Materials

Cerium dioxide nanoparticles were synthesized using laser ablation with a fiber-optic pulsed ytterbium laser (IPG Photonics, Laser Technologies Center, Saint Petersburg, Russia) equipped with the "High Contrast" option at a wavelength of 1.06 μm. The laser radiation intensity was 109 W/m^2, with a pulse duration of 200 μs and a repetition rate of up to 1 kHz [8]. Focused laser radiation was directed onto a cylindrical cerium dioxide target, causing ablated nanoparticles to be deposited onto monocrystalline silicon substrates positioned 10 mm from the target. Subsequently, the substrates with deposited cerium dioxide nanoparticles were dispersed ultrasonically in distilled water to form nanodispersed solutions.

Using sequential dispersion and centrifugation, seven samples of nanodispersed aqueous solutions of cerium dioxide nanoparticles (CeO_2) were prepared. Initially, a dispersive solution with a CDN concentration of 0.33 g/L was prepared and dispersed in an ultrasonic bath for 10 min at a power of 30 W. Subsequently, a 2 mL portion of the solution was transferred into a microtube and centrifuged for 5 min. To obtain Solution N1, a microcentrifuge was operated at a speed of 13,400 rpm. A 1.5 mL portion of the centrifuged solution from the upper part of the tube was transferred into a quartz cuvette for spectrophotometric analysis. Absorption spectra of the CeO_2 nanoparticles were recorded in the wavelength range of 200–400 nm to monitor their concentration in the solution. Solution N2 was prepared as follows: 1.5 mL of distilled water was added to the remaining 0.5 mL of the CDN solution in the microtube after the first centrifugation, then thoroughly mixed and dispersed again for 10 min. The contents of the microtube were centrifuged at a centrifuge speed of 10,000 rpm. Solutions N3–N6 were prepared using the same method but with different centrifugation speeds of 5000, 2000, 1000, and 800 rpm, respectively. For Solution N7, 1 mL of distilled water was added to the remaining 0.5 mL of the CDN solution, centrifuged at 800 rpm, mixed, and dispersed for 10 min. The optical densities of solutions N2–N7 were also recorded spectrophotometrically.

The sizes and morphology of ablated cerium dioxide particles in nanodispersed solutions were studied using an atomic force microscope SmartSPM™-1000. Ablated cerium dioxide nanoparticles from aqueous solutions N1–N7 were deposited onto monocrystalline silicon substrates using the drop-casting method. After the samples dried, the investigations were carried out. In the same way, studies were carried out on ablated cerium dioxide nanoparticles from the initial dispersed solution without sequential dispersion and centrifugation. The average sizes of homogeneous spherical ablated cerium dioxide nanoparticles in solutions N1–N7 were evaluated using small-angle X-ray scattering with the SAXSess mc^2 Anton Paar device. Optical spectra of the nanodispersed solutions were measured in the 200–700 nm range using a SF-2000 spectrophotometer. The narrow sub-bandgap widths in the forbidden band of the ablated CeO_2 nanoparticles for each of the seven solutions were determined using Tauc's method.

The influence of the size factor of ablated cerium dioxide nanoparticles obtained in systems N1–N7 on the efficiency of their antioxidant properties was investigated in the experiment. A spectrophotometric method was used to evaluate the presence and efficiency of the antioxidant properties of ablated CeO_2 nanoparticles during a photocatalytic reaction of the degradation of the organic dye methylene blue. The reaction was conducted in the presence of TiO_2 photocatalyst particles and ablated CeO_2 nanoparticles from dispersive solutions N1–N7. Methylene blue exists in both monomeric and dimeric forms, with the

monomer characterized by an absorption maximum at a wavelength of λ_{max} = 668 nm and the dimer by a maximum at λ_{max} = 612 nm.

The titanium dioxide used as a photocatalyst consisted of a chemically pure (99.9%) nanopowder with an average particle size of 75 ± 0.5 nm and an anatase crystal structure. Under exposure to ultraviolet light (30 W mercury lamp), titanium dioxide nanoparticles exhibited photocatalytic properties and efficiently degraded the methylene blue dye. The concentration of TiO_2 particles in the solution was 0.06 g/L. The TiO_2 particles were dispersed in an aqueous medium using an ultrasonic bath for 30 min. The nanodispersed solutions N1–N7 containing ablated cerium dioxide nanoparticles were also diluted twofold. Without dilution, the nanodispersed solutions exhibited highly effective antioxidant properties, making it challenging to identify the dependence of their antioxidant properties on particle size. The optical densities of the diluted solutions were then measured using a spectrophotometer in the wavelength range of 200–400 nm. The photocatalytic reaction was carried out for 60 min, with an MB volume of 70 µL in each cuvette. Subsequently, eight systems for photocatalysis were prepared, with their contents in the cuvettes detailed in Table 1.

Table 1. Composition of the systems in the cuvettes participating in the photocatalytic process.

System Number, N	Composition of Systems
0	1 mL H_2O + 1 mL solution TiO_2 + MB
1	1 mL solution N1 with CDN + 1 mL solution TiO_2 + MB
2	1 mL solution N2 with CDN + 1 mL solution TiO_2 + MB
3	1 mL solution N3 with CDN + 1 mL solution TiO_2 + MB
4	1 mL solution N4 with CDN + 1 mL solution TiO_2 + MB
5	1 mL solution N5 with CDN + 1 mL solution TiO_2 + MB
6	1 mL solution N6 with CDN + 1 mL solution TiO_2 + MB
7	1 mL solution N7 with CDN + 1 mL solution TiO_2 + MB

During the photocatalysis process, changes in the absorption spectra of MB in the visible wavelength range (550–750 nm) were recorded using an SF-2000 spectrophotometer.

3. Results and Discussion

Figure 1 shows the obtained AFM images of ablated cerium dioxide nanoparticles without sequential dispersion and centrifugation processes, as well as ablated cerium dioxide nanoparticles from dispersive solutions. The figure also includes size distribution histograms constructed based on the processing of the AFM images.

The presented histograms show that after the sequential alternation of ultrasonic dispersion and centrifugation processes, the particle size does not exceed 100 nm in contrast to the initial untreated solution, which exhibits a wide size distribution up to 200 nm. Table 2 presents the calculated average sizes of the ablated cerium dioxide nanoparticles.

Table 2. Average sizes of ablated cerium dioxide nanoparticles in the resulting solutions.

	Average Size							
N systems	original	1	2	3	4	5	6	7
d, nm	77 ± 0.5	30.4 ± 0.5	31.5 ± 0.5	32.7 ± 0.5	34 ± 0.5	35.3 ± 0.5	36.7 ± 0.5	38.2 ± 0.5

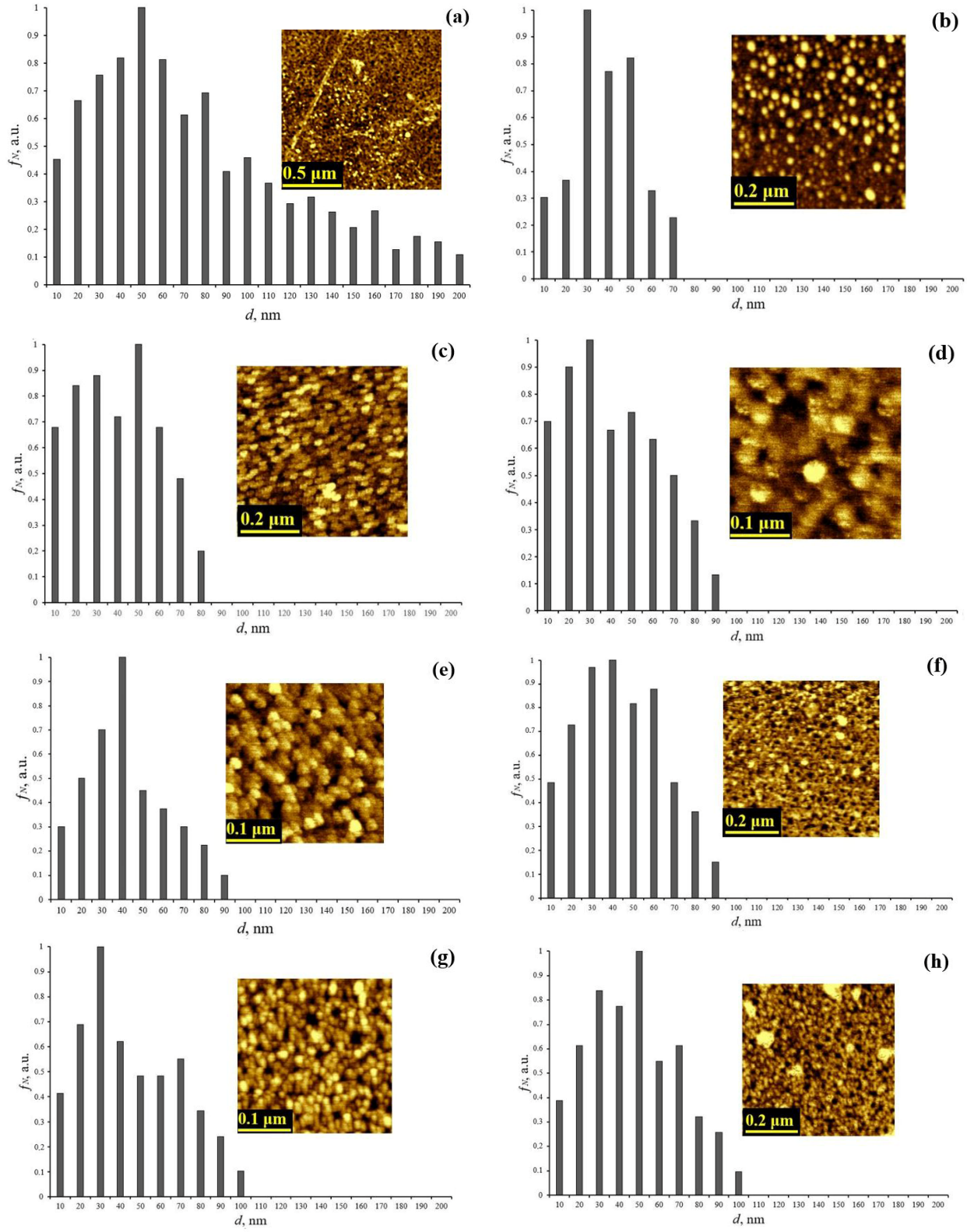

Figure 1. AFM image and granulometry of ablated cerium dioxide nanoparticles (**a**) from a dispersed solution without sequential dispersion and centrifugation; (**b**) from dispersed solution N1; (**c**) from dispersed solution N2; (**d**) from dispersed solution N3; (**e**) from dispersed solution N4; (**f**) from dispersed solution N5; (**g**) from dispersed solution N6; (**h**) from dispersed solution N7.

As shown in Table 2, the average sizes of CeO_2 nanoparticles range from 30.4 nm to 38.2 nm, confirming the effectiveness of the developed method for producing nanodispersed solutions with a narrow-size distribution.

The results of the small-angle X-ray scattering of cerium dioxide nanodispersed solutions prepared using the developed method are presented in Table 3.

Table 3. Average sizes of homogeneous spheres of ablated cerium dioxide nanoparticles in the obtained solutions.

Guinier Analysis for a Homogeneous Sphere							
N systems	1	2	3	4	5	6	7
d, nm	29.7 ± 0.2	32.1 ± 0.2	34.8 ± 0.2	37.8 ± 0.2	38.8 ± 0.2	39.7 ± 0.2	41.3 ± 0.2

The results of the study (Table 3) indicate that the method of sequential centrifugation produced systems of cerium dioxide nanodispersed solutions with a narrow-size distribution, characterized by varying average sizes of homogeneous spherical ablated cerium dioxide nanoparticles.

Figure 2 shows the dependence of the change in the electronic structure of ablated cerium dioxide nanoparticles on the size factor.

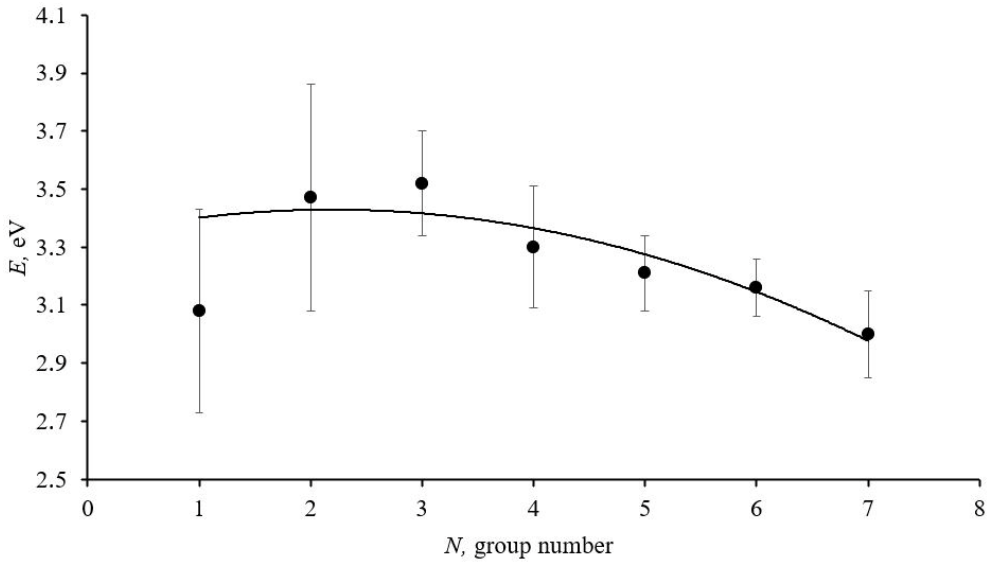

Figure 2. Graph of the dependence of the narrow bandgap width in the forbidden band of ablated cerium dioxide nanoparticles on their size. The solid line represents the approximating curve.

The graph presented in Figure 2 shows a decrease in the narrow sub-bandgap width in the forbidden band of ablated cerium dioxide nanoparticles as the average size of the homogeneous spheres increases, which aligns well with theoretical concepts.

The study of the antioxidant properties of nanodispersed solutions of cerium dioxide particles revealed that the residual concentration of methylene blue after photocatalysis was lowest in the system without the presence of ablated cerium dioxide nanoparticles compared to other systems. In this system, the oxidative degradation reaction of methylene blue proceeded by 18%. In systems containing nanodispersed solutions of ablated cerium dioxide nanoparticles, a reduction in the residual concentration of methylene blue by 13–15% was observed, which is attributed to the inactivation of reactive oxygen species in these systems.

After the photocatalytic reaction, the oxidation reaction rates were calculated for all systems. Subsequently, the reaction rates in systems containing cerium dioxide nanoparticles were determined by subtracting the reaction rate without cerium dioxide nanoparticles from the rates observed with nanoparticles, taking the rates with an opposite sign. The

resulting reaction rates were then normalized to the concentrations of the cerium dioxide nanodispersed solutions previously obtained. This approach was used to evaluate the antioxidant efficiency of ablated cerium dioxide nanoparticles for each size group.

Figure 3 presents a graph illustrating the dependence of the antioxidant activity of cerium dioxide nanodispersed solutions on the average size of the homogeneous spheres of ablated cerium dioxide nanoparticles in the obtained solutions.

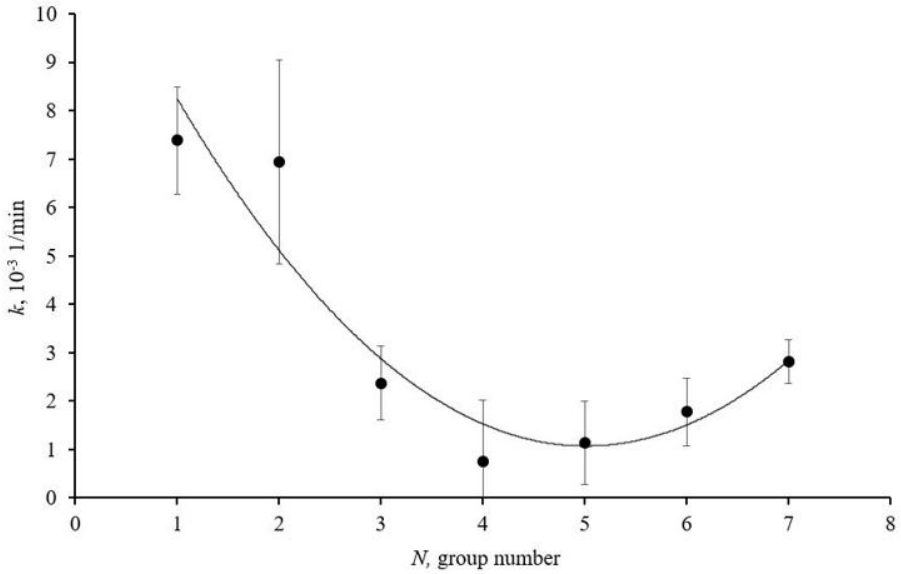

Figure 3. Antioxidant activity of size groups of ablated cerium dioxide nanoparticles in dispersed solutions N1–7 in photocatalytic reaction; solid line is approximating curve.

The graph (Figure 3) shows that sample N1 exhibits pronounced antioxidant properties. This is due to the high concentration of structural defects on the nanoparticle surfaces and the large specific surface area. The graph also indicates an increase in the antioxidant activity of samples N6 and N7. The reasons for this increase are associated with the high crystallinity of the particles and the reduction in the bandgap width.

4. Conclusions

Cerium dioxide nanoparticles with sizes ranging from 10 nm to several hundred nanometers were obtained using the laser ablation. A specialized sequential centrifugation technique was developed to produce nanodispersed solutions of ablated CeO_2 nanoparticles with a narrow-size distribution and varying average sizes. Atomic force microscopy and small-angle X-ray scattering were used to determine the average sizes of nanoparticles and homogeneous spheres of ablated cerium dioxide nanoparticles, which were found to vary within a narrow range, confirming the effectiveness of the developed methodology for obtaining nanodispersed solutions with a narrow-size distribution. Spectrophotometric analysis revealed that an increase in the average size of the homogeneous spheres of ablated cerium dioxide nanoparticles corresponds to a decrease in the narrow sub-bandgap width in the forbidden band.

The investigation of the antioxidant properties of the obtained nanodispersed solutions revealed that the sample with an average homogeneous sphere size of 29.7 nm exhibits pronounced antioxidant properties. This is attributed to the high concentration of structural defects on the nanoparticle surfaces and their large specific surface area. Additionally, the antioxidant activity increases for samples with average homogeneous sphere sizes of 39.7 nm and 41.3 nm. The enhanced antioxidant activity of these size groups is associated with the increased crystallinity of the particles and the reduction in their bandgap width.

Author Contributions: Conceptualization V.M. and M.P.; methodology V.M.; validation M.P., P.S., and R.K.R.; formal analysis V.M., M.P., and P.S.; investigation V.M. and M.P.; data curation M.P. and R.K.R.; writing—original draft preparation, V.M. and M.P.; writing—review and editing V.M., M.P., P.S., and R.K.R. All authors have read and agreed to the published version of the manuscript.

Funding: The study was carried out with the financial support of the Ministry of Science and Higher Education of the Russian Federation (agreement no. 075-03–2025–526).

Institutional Review Board Statement: Not applicable.

Informed Consent Statement: Not applicable.

Data Availability Statement: Data are contained within the article.

Conflicts of Interest: The authors declare no conflicts of interest.

Abbreviations

The following abbreviations are used in this manuscript:

AFM	Atomic Force Microscope
SAXS	Small-Angle X-ray Scattering
ROS	Reactive Oxygen Species
CDN	Cerium Dioxide Nanoparticles
MB	Methylene Blue

References

1. Abdulsattar, S.A. Cerium Oxide Nanoparticles Role as Antioxidant. *Med. J. Babylon* **2024**, *21*, 235–239. [CrossRef]
2. Calvache-Muñoz, J.; Prado, F.A.; Tirado, L.; Daza-Gomez, L.C.; Cuervo-Ochoa, G.; Calambas, H.L.; Rodríguez-Páez, J.E. Structural and optical properties of CeO_2 nanoparticles synthesized by modified polymer complex method. *J. Inorg. Organomet. Polym. Mater.* **2019**, *29*, 813–826. [CrossRef]
3. Abid, S.A.; Taha, A.A.; Ismail, R.A.; Mohsin, M.H. Antibacterial and cytotoxic activities of cerium oxide nanoparticles prepared by laser ablation in liquid. *Environ. Sci. Pollut. Res.* **2020**, *27*, 30479–30489. [CrossRef] [PubMed]
4. Reed, K.; Bush, N.; Burns, Z.; Doherty, G.; Foley, T.; Milone, M.; Cromer, M. Modeling the kinetic behavior of reactive oxygen species with cerium dioxide nanoparticles. *Biomolecules* **2019**, *9*, 447. [CrossRef] [PubMed]
5. Khashan, K.S.; Badr, B.A.; Sulaiman, G.M.; Jabir, M.S.; Hussain, S.A. Antibacterial activity of Zinc Oxide nanostructured materials synthesis by laser ablation method. *J. Phys. Conf. Ser.* **2021**, *1795*, 012040. [CrossRef]
6. Brandão Da Silva Assis, M.; Nestal De Moraes, G.; De Souza, K.R. Cerium oxide nanoparticles: Chemical properties, biological effects and potential therapeutic opportunities. *Biomed. Rep.* **2024**, *20*, 48. [CrossRef]
7. Mamontov, V.A.; Ryzhenkova, A.Y.; Pugachevskii, M.A. Characterization of size and morphological composition of ablated nanoparticles of cerium dioxide after ultrasonic dispersion and centrifugation in aqueous solution. *J. Phys. Conf. Ser.* **2021**, *2064*, 012083. [CrossRef]
8. Pugachevskii, M.A.; Chibisov, A.N.; Mamontov, V.A.; Kuzmenko, A.P. Antioxidant properties of stabilized CeO_2 nanoparticles. *Phys. Status Solidi (A)* **2021**, *218*, 2100355. [CrossRef]
9. Pugachevskii, M.A.; Mamontov, V.A.; Syuy, A.V.; Kuzmenko, A.P. Effect of pH on antioxidant properties of ablated CeO_2 nanoparticles in photocatalytic process. *J. Ind. Eng. Chem.* **2022**, *106*, 74–76. [CrossRef]
10. Pugachevskii, M.A.; Mamontov, V.A.; Aung, N.V.; Chekadanov, A.S.; Kuzmenko, A.P. Production of Ablated CeO_2 Particles with Nanodispersed Compositional Distribution. *Tech. Phys. Lett.* **2020**, *46*, 1032–1035. [CrossRef]

Disclaimer/Publisher's Note: The statements, opinions and data contained in all publications are solely those of the individual author(s) and contributor(s) and not of MDPI and/or the editor(s). MDPI and/or the editor(s) disclaim responsibility for any injury to people or property resulting from any ideas, methods, instructions or products referred to in the content.